Title

PRUNE2 is a human prostate cancer suppressor regulated by the intronic long noncoding RNA PCA3

Journal

Proceedings of the National Academy of Sciences of the United States of America, 112(27)

ISSN

0027-8424

Authors

Salameh, Ahmad
Lee, Alessandro K
Cardó-Vila, Marina
et al.

Publication Date

2015-07-07

DOI

10.1073/pnas.1507882112

Peer reviewed

PRUNE2 is a human prostate cancer suppressor regulated by the intronic long noncoding RNA *PCA3*

Ahmad Salameh[a,b,1], Alessandro K. Lee[a,1,2], Marina Cardó-Vila[a,c,d,e], Diana N. Nunes[a,f], Eleni Efstathiou[a,g], Fernanda I. Staquicini[a,c,d,e], Andrey S. Dobroff[a,c,d,e], Serena Marchiò[h], Nora M. Navone[a,g], Hitomi Hosoya[a,3], Richard C. Lauer[c,e,i], Sijin Wen[j,4], Carolina C. Salmeron[a,c,d,e], Anh Hoang[a,g], Irene Newsham[a], Leandro A. Lima[f], Dirce M. Carraro[f], Salvatore Oliviero[k], Mikhail G. Kolonin[b], Richard L. Sidman[l], Kim-Anh Do[j], Patricia Troncoso[a,m], Christopher J. Logothetis[a,g], Ricardo R. Brentani[f,5], George A. Calin[n,o], Webster K. Cavenee[p,6], Emmanuel Dias-Neto[a,f,q,6,7], Renata Pasqualini[a,c,d,e,g,6,7], and Wadih Arap[a,c,e,g,i,6,7]

[a]David H. Koch Center for Applied Research of Genitourinary Cancers, The University of Texas M.D. Anderson Cancer Center, Houston, TX 77030; [b]Brown Foundation Institute of Molecular Medicine, University of Texas Health Science Center at Houston, Houston, TX 77030; [c]University of New Mexico Cancer Center, University of New Mexico School of Medicine, Albuquerque, NM 87131; [d]Division of Molecular Medicine, University of New Mexico School of Medicine, Albuquerque, NM 87131; [e]Department of Internal Medicine, University of New Mexico School of Medicine, Albuquerque, NM 87131; [f]International Research Center, A.C. Camargo Cancer Center, São Paulo, SP 01508-010 Brazil; [g]Department of Genitourinary Medical Oncology, The University of Texas M.D. Anderson Cancer Center, Houston, TX 77030; [h]Candiolo Cancer Institute and Department of Oncology, University of Turin, Candiolo 10060, Italy; [i]Division of Hematology/Oncology, University of New Mexico School of Medicine, Albuquerque, NM 87131; [j]Department of Biostatistics, The University of Texas M.D. Anderson Cancer Center, Houston, TX 77030; [k]Human Genetics Foundation, Torino 10126, Italy; [l]Harvard Medical School and Department of Neurology, Beth Israel Deaconess Medical Center, Boston, MA 02215; [m]Department of Pathology, The University of Texas M.D. Anderson Cancer Center, Houston, TX 77030; [n]Department of Experimental Therapeutics, The University of Texas M.D. Anderson Cancer Center, Houston, TX 77030; [o]Center for RNA Interference and Noncoding RNA, The University of Texas M.D. Anderson Cancer Center, Houston, TX 77030; [p]Ludwig Institute for Cancer Research, University of California-San Diego, La Jolla, CA 92093; and [q]Institute of Psychiatry, University of São Paulo Medical School, São Paulo 01060, Brazil

Edited by Owen N. Witte, Howard Hughes Medical Institute, University of California, Los Angeles, CA, and approved May 13, 2015 (received for review March 16, 2015)

***Prostate cancer antigen 3* (*PCA3*) is the most specific prostate cancer biomarker but its function remains unknown. Here we identify *PRUNE2*, a target protein-coding gene variant, which harbors the *PCA3* locus, thereby classifying *PCA3* as an antisense intronic long noncoding (lnc)RNA. We show that *PCA3* controls PRUNE2 levels via a unique regulatory mechanism involving formation of a *PRUNE2/PCA3* double-stranded RNA that undergoes adenosine deaminase acting on RNA (ADAR)-dependent adenosine-to-inosine RNA editing. *PRUNE2* expression or silencing in prostate cancer cells decreased and increased cell proliferation, respectively. Moreover, *PRUNE2* and *PCA3* elicited opposite effects on tumor growth in immunodeficient tumor-bearing mice. Coregulation and RNA editing of *PRUNE2* and *PCA3* were confirmed in human prostate cancer specimens, supporting the medical relevance of our findings. These results establish *PCA3* as a dominant-negative oncogene and *PRUNE2* as an unrecognized tumor suppressor gene in human prostate cancer, and their regulatory axis represents a unique molecular target for diagnostic and therapeutic intervention.**

PRUNE2 | *PCA3* | long noncoding RNA | ADAR | prostate cancer

Several lines of evidence demonstrate that long noncoding RNAs (lncRNAs) are functional in carcinogenesis through regulatory mechanisms such as promoter looping, alternative splicing, antisense gene silencing, transcriptional regulation, and DNA repair, thus potentially serving as tumor markers. A few lncRNA species have emerged as potential prostate cancer biomarkers such as *prostate cancer gene expression marker-1* (*PCGEM1*) and *prostate cancer noncoding RNA1* (*PRNCR1*), which enhance androgen receptor (AR)-dependent gene activation, and *prostate cancer-associated ncRNA transcript-1* (*PCAT1*), which silences *BRCA2* via posttranscriptional homologous recombination (1). Notably, the most specific biomarker in human prostate cancer identified to date is an lncRNA, *prostate cancer antigen 3* (*PCA3*, also known as $PCA3^{DD3}$ or $DD3^{PCA3}$), which is up-regulated in human prostate cancer (2). Since its discovery more than 15 y ago, *PCA3* has been extensively investigated (3) and has been approved for clinical applications to aid the diagnosis of prostate cancer in both the European Union and the United States. Paradoxically—despite its striking clinical specificity—the inherent cellular role of the lncRNA *PCA3* in human prostate cancer, if any, remains completely unknown (1). Here we report a unique biological function for *PCA3*. Within a single functional genetic unit, we show that *PCA3* is an antisense intronic lncRNA that down-regulates an as yet unrecognized tumor suppressor gene, a human homolog of the *Drosophila* prune gene, *PRUNE2*, through a process that involves RNA editing mediated by a supramolecular complex containing adenosine deaminase acting on RNA (ADAR) family members. We propose a working model in which *PCA3* acts as a dominant-negative oncogene in prostate cancer and show consistent results in therapeutic preclinical models and in patient-derived human samples. Therefore, the molecular interaction of *PRUNE2* and *PCA3* is a candidate target for translational applications.

Results

PCA3 Is an Antisense Intronic lncRNA Within a Single _PRUNE2_ Transcriptional Unit. Certain mammalian lncRNAs are embedded in the intronic-antisense regions of protein-coding genes (4–6).

Author contributions: A.S., A.K.L., M.C.-V., D.N.N., E.E., F.I.S., A.S.D., E.D.-N., R.P., and W.A. designed research; A.S., A.K.L., M.C.-V., D.N.N., F.I.S., A.S.D., H.H., A.H., and E.D.-N. performed research; E.E., S.M., N.M.N., R.C.L., S.W., C.C.S., D.M.C., S.O., M.G.K., R.L.S., K.-A.D., P.T., C.J.L., R.R.B., and G.A.C. contributed new reagents/analytic tools; A.S., A.K.L., M.C.-V., D.N.N., E.E., F.I.S., A.S.D., H.H., R.C.L., S.W., C.C.S., I.N., L.A.L., M.G.K., R.L.S., K.-A.D., P.T., C.J.L., R.R.B., G.A.C., W.K.C., E.D.-N., R.P., and W.A. analyzed data; A.S., A.K.L., M.C.-V., D.N.N., E.E., F.I.S., A.S.D., R.L.S., G.A.C., W.K.C., E.D.-N., R.P., and W.A. wrote the paper; and E.D.-N., R.P., and W.A. jointly supervised this project.

Conflict of interest statement: The University of New Mexico has filed patents on the technology and intellectual property reported here. If licensing or commercialization occurs, the researchers (A.S., A.K.L., D.N.N., E.D.-N., R.P., and W.A.) are entitled to standard royalties.

This article is a PNAS Direct Submission.

Freely available online through the PNAS open access option.

Data deposition: The sequences reported in this paper have been deposited in the GenBank database (accession nos. FJ808772, FJ808773, and AF103907).

[1]A.S. and A.K.L. contributed equally to this work.

[2]Present address: Janssen-Cilag SpA., Cologno Monzese, Milan 20093, Italy.

[3]Present address: The US Naval Hospital Yokosuka, PSC 475 FPO AP 96350-9998, Japan.

[4]Present address: School of Public Health, West Virginia University, Morgantown, WV 26506.

[5]Deceased November 29, 2011.

[6]To whom correspondence may be addressed. Email: wcavenee@ucsd.edu, emmanuel@cipe.accamargo.org.br, rpasqual@salud.unm.edu, or warap@salud.unm.edu.

[7]E.D.-N., R.P., and W.A. contributed equally to this work.

This article contains supporting information online at www.pnas.org/lookup/suppl/doi:10.1073/pnas.1507882112/-/DCSupplemental.

Significance

Prostate cancer has an unpredictable natural history: While most tumors are clinically indolent, some patients display lethal phenotypes. Serum prostate-specific antigen is the most often used test in prostate cancer but screening is controversial. Treatment options are limited for metastatic disease, hence the need for early diagnosis. Prostate cancer antigen 3 (*PCA3*), a long noncoding RNA, is the most specific biomarker identified and approved as a diagnostic test. However, its inherent biological function (if any) has remained elusive. We uncovered a negative transdominant oncogenic role for *PCA3* that down-regulates an unrecognized tumor suppressor gene, *PRUNE2* (a human homolog of the *Drosophila* prune gene) thereby promoting malignant cell growth. This work defines a unique biological function for *PCA3* in prostate cancer.

PCA3 is a spliced intronic antisense lncRNA embedded within intron 6 of the corresponding sense gene *PRUNE2* (2, 7–10) (Fig. 1*A*). We hypothesized the existence of a functional role between *PCA3* and PRUNE2, and their involvement in prostate cancer progression. To study this possibility, we investigated *PRUNE2* as well as the *PCA3* intronic antisense transcripts, which we cloned from MDA-PCa-133, a patient-derived xenograft (PDX) of bone metastasis from prostate cancer (11) (Fig. 1 *A* and *B*). We next analyzed the expression of *PRUNE2* in representative panels of human tumors and nonmalignant cell lines by quantitative gene expression profiling with primers located in the *PRUNE2* exons that flank *PCA3* (Tables S1 and S2 and Fig. S1 *A* and *B*). *PRUNE2* was detectable in prostate cancer cell lines, with the highest levels in androgen-dependent (LNCaP) cells, as well as in several brain and breast lines. We also analyzed *PRUNE2* levels alongside *PCA3* lncRNA in prostate cancer cells and observed differential expression of the two genes: LNCaP cells displayed the highest levels of both *PRUNE2* and *PCA3* relative to androgen-independent (DU145 and PC3) cells (Fig. S1*C*). We confirmed the expression of native or recombinant V5-tagged PRUNE2 by immunoblot analysis, and the predicted endogenous protein (~337 kDa) was observed in LNCaP but not in PC3 cells (Fig. S1 *D* and *E*).

***PCA3* lncRNA Binds *PRUNE2* Pre-mRNA and Regulates Its Levels.** Given that *PCA3* is embedded within intron 6 of *PRUNE2*, and is transcribed in the antisense direction, we hypothesized that a double-stranded (ds)RNA forms between *PCA3* lncRNA and *PRUNE2* pre-mRNA to regulate PRUNE2 levels in prostate cancer. To evaluate this possibility, we first generated prostate cancer cell lines (LNCaP and PC3) stably transduced with ectopic *PCA3*, *PCA3*-shRNA, ectopic *PRUNE2*, *PRUNE2*-shRNA, or the corresponding controls. Levels of endogenous PRUNE2 protein, pre-mRNA and mRNA increased with *PCA3* silencing and decreased with ectopic *PCA3* expression (Fig. 1 *C* and *D* and Fig. S1 *F–H*). We confirmed these findings in prostate- and prostate cancer-derived cells, where ectopic *PCA3* expression induced down-regulation of endogenous PRUNE2 expression (Fig. S2*A*). To determine whether *PRUNE2* and *PCA3* form a dsRNA, we used co-RNA-FISH assays. *PCA3* and *PRUNE2* hybridized in the same nuclear foci (Fig. 1*E* and Fig. S2*A*). These foci were completely depleted on treatment with RNase III, which degrades only dsRNA, but not with RNase A, which degrades only single-stranded (ss)RNA (Fig. 1*E* and Fig. S2*B*), indicating the formation of dsRNA from the physical association of *PCA3* and *PRUNE2* pre-mRNA. Next, to evaluate whether binding of *PRUNE2* mRNA to *PCA3* was required for the regulation of PRUNE2 levels, we assessed the effect of *PCA3* on exogenous mature *PRUNE2* cDNA, which has no sequence complementarity to *PCA3* and therefore would be unable to form a dsRNA. Indeed, ectopic *PCA3* did not affect the exogenous expression of PRUNE2 mRNA and protein (Fig. S3*A*). To complement this finding, we also designed and expressed a *PRUNE2* construct that contains no protein-coding sequence but is still fully complementary to *PCA3* (termed intron6-*PRUNE2*) and should therefore be able to bind *PCA3* and possibly sequester it from *PRUNE2*. Consistent with this, overexpression of intron6-*PRUNE2* caused an increase in endogenous *PRUNE2* mRNA in the cytoplasm and a concomitant reduction in the nucleus (Fig. 1*F*). We confirmed a direct interaction between *PCA3* and its corresponding antisense sequence (intron6-*PRUNE2*) by using RNase-resistant assays and co-RNA-FISH in tumor cells expressing both sequences (Fig. S3 *B–E*). These data suggest that *PCA3* binding to *PRUNE2* pre-mRNA controls PRUNE2 levels.

ADARs Bind *PRUNE2/PCA3* dsRNA and Regulate PRUNE2 Levels. ADAR proteins are key regulatory enzymes for RNA editing and sequestering of noncoding RNA sequences, such as introns and untranslated mRNAs (5, 11–13), derived from the hybridization of retroinverted Alu elements (5, 13), with conversion of adenosine-to-inosine (A-to-I) RNA editing after nuclear dsRNA formation. Thus, we hypothesized that *PCA3-PRUNE2* dsRNA may be regulated by ADAR-mediated RNA editing. To test this possibility, we used quantitative RT-PCR (qRT-PCR), co-RNA-FISH, and RNA-ChIP. We found that endogenous *PCA3* and *PRUNE2* pre-mRNAs colocalize to nuclear foci associated with

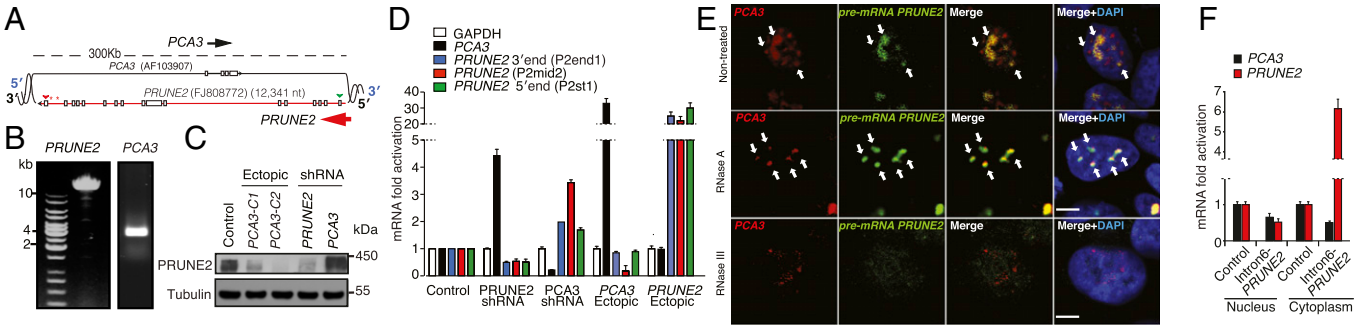

Fig. 1. *PRUNE2/PCA3* cloning, genomic structure, and colocalization. (*A*) Genomic context of intron/exon boundaries of *PCA3* and *PRUNE2* (GenBank accession no. FJ808772). Stars indicate missing or new exons; arrowheads indicate initiation (green) or stop (red) codons. Arrows indicate transcript orientation (black, *PCA3*; red, *PRUNE2*). (*B*) RT-PCR with RNA from the PDX MDA-PCa-133 used to clone/sequence *PRUNE2*. (*C*) Analysis of PRUNE2 in LNCaP cells stably expressing ectopic *PCA3*, *PCA3*-silenced, *PRUNE2*-silenced, or control. (*D*) qRT-PCR assays with primers (Table S1) amplifying *PCA3* or different regions of *PRUNE2* in LNCaP cells with silenced or ectopic *PRUNE2* and *PCA3*. (*E*) Combined RNase resistance and RNA-FISH analysis. Before hybridization, LNCaP cells were treated with RNase A or RNase III. Hybridization was performed with specific probes against *PCA3* and *PRUNE2* transcripts. Nuclei are stained with DAPI. Arrows indicate foci. Confocal images are shown (bar, 10 μm). Fig. 1*E* represents 100× magnifications (from Fig. S3*A*). (*F*) Expression effects of intron6-*PRUNE2* on nuclear and cytoplasmic *PCA3* and *PRUNE2* levels in LNCaP cells. Shown data are mean ± SD.

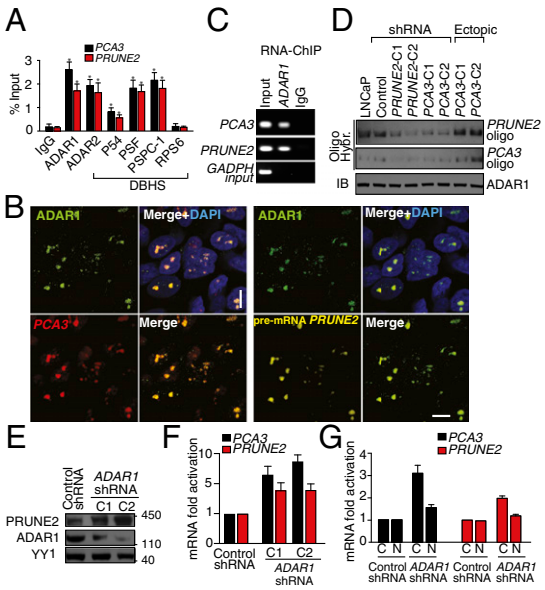

Fig. 2. *PRUNE2/PCA3* colocalization to ADAR1. (*A*) RNA-ChIP and *PCA3* and *PRUNE2* binding by qRT-PCR in LNCaP cells. (*B*) Combined RNase resistance and RNA-FISH analysis. Before hybridization, LNCaP cells were treated with RNase A. Hybridization and immunostaining were performed with specific probes and an anti-ADAR1 antibody. (*C*) *PCA3* and *PRUNE2* binding to ADAR1 by RNA-ChIP. (*D*) Hybridization with biotin-labeled oligomers (Table S1) against *PCA3* and *PRUNE2* in LNCaP cells after UV-induced RNA-protein cross-linking. Immunoblot against ADAR1 is shown. (*E* and *F*) Evaluation of *PCA3* and PRUNE2 expression in LNCaP cells stably expressing two independent lentiviral *ADAR1*-shRNAs: immunoblots against PRUNE2, ADAR1, and control protein (YY1) (*E*) and qRT-PCR (*F*) are shown. (*G*) Cytosolic (C) and nuclear (N) RNA fractionation followed by qRT-PCR; specific oligonucleotides served for amplification of nuclear pre-mRNA and cytosolic mRNA of *PCA3* and *PRUNE2*. Shown data are mean ± SD. $*P < 0.05$; $**P < 0.01$.

ADAR proteins, which were sensitive to RNase III treatment (Fig. 2 *A–C* and Fig. S4). *PRUNE2/PCA3* dsRNA and ADAR1 formed a complex only when both RNA species were coexpressed; the corresponding signals for *PRUNE2/PCA3* dsRNA decreased after *PCA3* or *PRUNE2* silencing and increased with ectopic expression of *PCA3* in a UV-induced RNA-protein cross-linking assay (Fig. 2*D*). To determine whether ADAR proteins regulate *PRUNE2* and *PCA3* levels, we silenced *ADAR1* in human tumor cells and found increased *PRUNE2* mRNA and protein levels (Fig. 2 *E–G*). We also found that ADAR-depleted prostate cancer cells have increased cytosolic *PRUNE2* and *PCA3* levels (Fig. 2 *F* and *G* and Fig. S5 *A* and *B*), revealing the importance of ADAR members in the regulation of both genes, consistent with functions of A-to-I editing in the regulation of noncoding RNA species (14). To gain functional insight into the regulation of *PRUNE2* and *PCA3*, we established sensor/reporter assays in which either *PCA3* or the *PCA3* antisense sequence (i.e., intron6-*PRUNE2*) was fused to reporters to generate *PCA3-luciferase* or *intron6-PRUNE2-GFP*. Reporter expression (by FACS and luminescence assays) showed that the coexpression of intron6-*PRUNE2-GFP* plus *PCA3* or intron6-*PRUNE2* plus *PCA3-luciferase* results in reduction of the corresponding reporter signals compared to controls (Fig. S5 *A–F*). Thus, in addition to *PCA3* regulating *PRUNE2* levels, and consistent with our earlier results, intron6-*PRUNE2* could also down-regulate *PCA3* (Fig. 1*F*). Silencing of ADAR1 or ADAR2 increased the reporter signals, confirming that these enzymes are required for a coregulatory effect on both RNAs (Fig. S5 *E–H*).

RNA Editing of *PRUNE2* and *PCA3* RNA Species. Our results thus far have indicated that ADAR proteins associate with *PRUNE2/PCA3* dsRNA and regulate *PRUNE2* and *PCA3* levels via A-to-I RNA editing. To test this possibility directly, we evaluated the presence of A-to-I editing throughout the genomic coordinates of *PCA3* and its corresponding antisense pre-mRNA intron6-*PRUNE2* by RNA capture followed by next-generation sequencing. Although RNA editing is found largely within Alu elements, we carefully filtered out repetitive elements (such as Alu sequences) to avoid erroneous alignments. We showed that A > G/T > C changes, which reflect A-to-I editing, were the most frequent substitutions. Editing sites were distributed in intronic and exonic

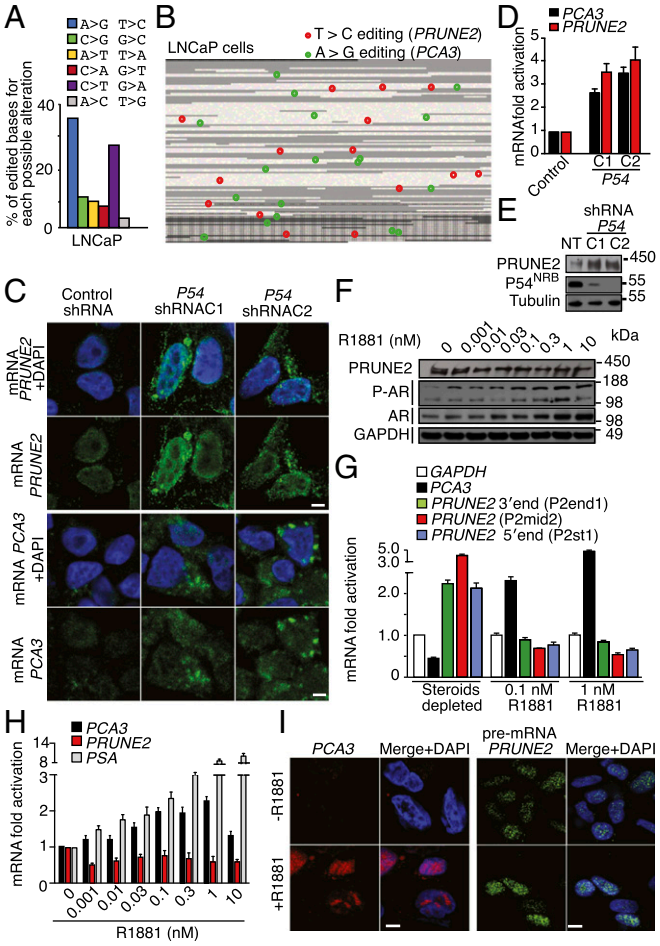

Fig. 3. Functional role of RNA editing and androgen receptor (AR) activation in PRUNE2/*PCA3* regulation. (*A* and *B*) Identification, quantification, and distribution of A > G/T > C changes (features pathognomonic of A-to-I editing in both strands of the *PRUNE2/PCA3* dsRNA) analyzed after RNA capture followed by high-throughput sequencing. Reads were aligned against hg19 of the region. Only nondbSNP variations indicated by at least three reads, and out of repetitive elements were considered. (*A*) Distribution and percentage of all possible alterations for the *PCA3* genomic coordinates in LNCaP cells are shown. (*B*) RNA editing map for LNCaP cells showing the precise location of each A > G (green) or T > C (red) sites over *PCA3* and intron6-*PRUNE2* pre-mRNA species. Each square represents one individual base from the *PCA3* locus (23,112 nt). Black borders delimit the bases of the four annotated exons (3,923 nt). Repeats (RepeatMasker) are shown in gray (*B*). (*C–E*) Evaluation of *PCA3* and *PRUNE2* levels in LNCaP cells stably expressing two independent P54^{NRB}-shRNA clones (C1 and C2) or controls (NT). Detection of *PCA3* and *PRUNE2* mRNA cytosolic levels by RNA-FISH (*C*) and by qRT-PCR (*D*) are shown. Analysis of PRUNE2 expression in LNCaP P54^{NRB}-silenced cells or negative control is shown (*E*). (*F*) Analysis of PRUNE2, AR, and phosphorylated AR (P-AR) expression in after concentration-dependent androgen stimulation with R1881. Representative PAGE 3–8% shown. (*G*) Relative mRNA expression levels of *PCA3* and *PRUNE2* transcript under R1881 stimulation. (*H*) Relative mRNA expression of *PRUNE2*, *PCA3*, and *PSA* (positive control) measured by qRT-PCR in LNCaP cells after dose-dependent R1881 stimulation. (*I*) RNA-FISH analysis for *PCA3* and pre-mRNA of *PRUNE2* in LNCaP cells under steroid-depleted conditions or after androgen stimulation.

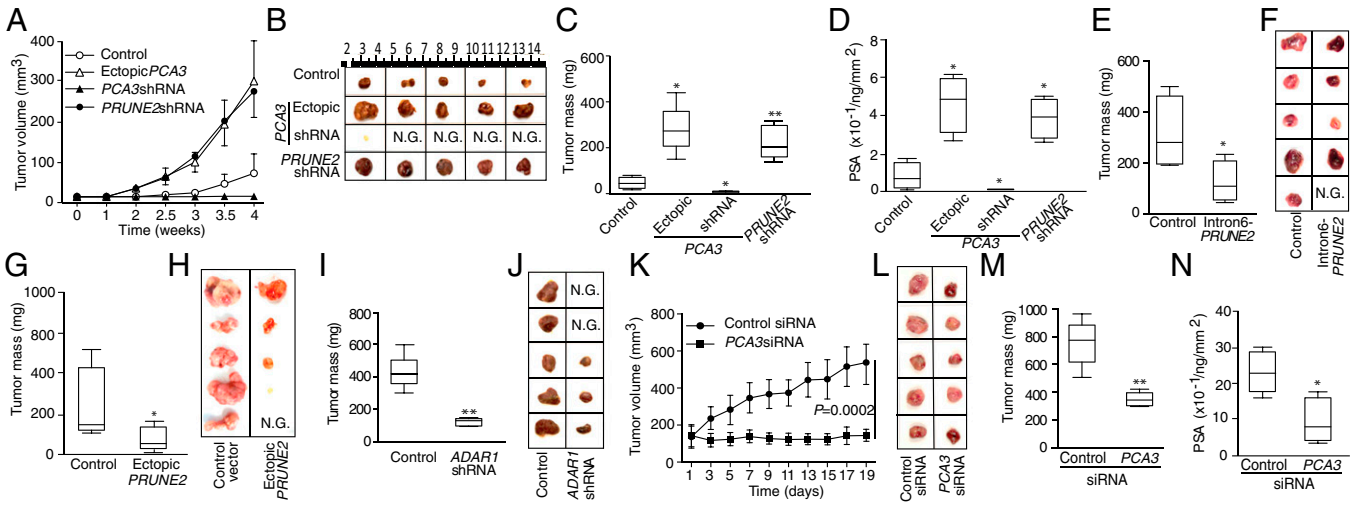

Fig. 4. PRUNE2/*PCA3* functions in tumor xenograft models of prostate cancer. (*A–D*) Male SCID mice received SC injection of 5×10^6 LNCaP cells stably expressing ectopic *PCA3*, *PCA3*-silenced, *PRUNE2*-silenced, or negative controls. Tumor growth was monitored and volume was measured (*A*). Tumors are shown after 4 wk (*B*); tumor mass (*C*) and serum PSA concentration (*D*) were determined. (*E* and *F*) Tumor growth in mice bearing LNCaP xenografts from cells stably expressing intron6-*PRUNE2* (antisense sequence to *PCA3*) or controls. Tumor growth in SCID mice bearing PC3 xenografts of cells stably expressing either ectopic PRUNE2 or negative controls (*G* and *H*) and LNCaP cells stably expressing *ADAR1*-shRNA or negative controls (*I* and *J*). (*K–N*) *PCA3* silencing in vivo by targeting SCID mice bearing LNCaP xenografts of cells stably expressing ectopic *PCA3* constructs. Two cohorts of SCID mice with size-matched tumors ($n = 10$/group) received 8 μg of stealth chemically modified *PCA3*-siRNA or negative control-siRNA per dose; treatments and controls received a series of doses ($n = 9$) through alternating intratumoral or i.p. administration every other day. Tumor volumes, measured before each administration, were plotted over time (*K*), and representative tumors at the experimental end point are shown (*L*). Tumor xenograft mass (*M*) and serum PSA concentration (*N*) were determined at the end point. In each experiment, 6–10 mice per group were treated. N.G., no growth. Mean ± SD is shown. $^*P < 0.05$, $^{**}P < 0.01$.

regions (Fig. 3 *A* and *B*), suggesting that a dsRNA hybrid is formed between pre-mRNA species of both genes, as observed in the RNA colocalization experiments. Given that the *Drosophila* behavior human splicing (DBHS) protein $P54^{NRB}$ preferentially binds to inosine-containing RNA (RNA-I) and regulates gene expression, we investigated a potential role for $P54^{NRB}$ and other DBHS proteins in regulating *PRUNE2*/*PCA3*. Both, *PCA3* and *PRUNE2* pre-mRNA species associated with $P54^{NRB}$ and the other two known mammalian family members (PSF and PSPC-1) compared with negative control RNA by RNA-ChIP (Fig. 2*A*) or combined co-RNA-FISH and immunofluorescence assays (Fig. S6). In addition, $P54^{NRB}$-silenced prostate cancer cells had increased levels of *PCA3* and *PRUNE2* mature RNA (Fig. 3 *C* and *D*) and a concomitant increase of PRUNE2 protein levels relative to controls (Fig. 3*E*). These data confirm that *PRUNE2* and *PCA3* RNAs undergo A-to-I editing and reveal a functional role for DBHS proteins in their regulation.

Function of the *PRUNE2*/*PCA3* Regulatory Axis in Prostate Cancer. Androgen dependence and resistance to androgen deprivation therapy are central to the biological and clinical features of prostate cancer. Thus, we investigated whether AR activation regulates *PCA3* and *PRUNE2* expression in androgen-dependent LNCaP cells, which had lower *PCA3* and higher *PRUNE2* levels than androgen-independent PC3 cells, when grown in steroid-depleted serum (Fig. 3 *F* and *G* and Fig. S1*C*). Androgen stimulation of LNCaP cells with a synthetic testosterone homolog (R1881) induced a concomitant increase of *PCA3* and decrease of *PRUNE2* levels (Fig. 3 *F–H*), consistent with a report that *PCA3* modulates prostate cancer through AR signaling (15). We also observed an increase in nuclear localization of *PRUNE2* and *PCA3* along with androgen-induced responses (Fig. 3*I*). Thus, *PRUNE2*/*PCA3* regulation appears to be sensitive to AR activation, a molecular hallmark of prostate cancer. To further assess the functional role(s) of the *PRUNE2*/*PCA3* regulatory axis in prostate cancer, we generated LNCaP cells (PRUNE2-expressing) or PC3 cells (PRUNE2-deficient) stably expressing lentiviral constructs to silence or ectopically express *PRUNE2* and *PCA3* (Figs. S1 *D–F* and S3*A*). *PCA3* silencing or ectopic *PRUNE2* expression decreased cell proliferation and transformation in vitro; in contrast, *PRUNE2* silencing or ectopic *PCA3* expression increased cell proliferation and transformation (Figs. S7 and S8 *A–C*). Moreover, ectopic expression of *PCA3* or antisense *PCA3* (*intron6-PRUNE2*), which downregulates *PCA3*, respectively decreased and increased endogenous, with no effect on exogenous mature *PRUNE2* expression lacking complementarity with *PCA3* (Fig. 1*C* and Figs. S2*A* and S8 *D* and *E*). Finally, we found that PRUNE2-deficient PC3 cells stably expressing ectopic *PRUNE2* had lower levels of proliferation and transformation in vitro (Fig. S8 *A* and *C*). These results are consistent with the negative regulation of *PRUNE2* by *PCA3*. We next investigated the downstream molecular mechanism(s) through which PRUNE2 suppresses tumor growth. PRUNE2 has three predicted functional domains (15): BCH, DHHA2, and PPX1 (Fig. S9*A*). BCH inhibits RhoA, a small GTPase that regulates the cytoskeleton, cell adhesion, and migration (16), whereas DHHA2 interacts with Nm23-H1, a metastasis suppressor (17). We found that endogenous PRUNE2 coimmunoprecipitates with RhoA and Nm23-H1 (Fig. S9 *B–D*). Consistent with an inhibitory role for *PRUNE2* in RhoA signaling, PRUNE2 levels increased when LNCaP cells were grown in nonadherent culture conditions (Fig. S9*E*), and the distribution of PRUNE2 was inversely correlated with focal adhesion sites in LNCaP-derived spheroids (Fig. S9 *C* and *F*). In addition, we observed alterations in tumor cell adhesion and spreading, but no effect on apoptosis (Fig. S10 *A–D*). We also noted decreased adhesion, spreading, and migration of prostate cancer cells upon PRUNE2 expression and the opposite effect on ectopic expression of *PCA3* or PRUNE2 silencing (Fig. S10 *E–J*). These results, along with the established functions of interacting proteins (16–18), suggest that PRUNE2 primarily decreases tumor growth by inhibiting cell proliferation but also affects adhesion, spreading, and migration. We subsequently extended these results to human tumor xenograft models; LNCaP prostate cancer cells stably expressing *PRUNE2*-shRNA, ectopic *PCA3*, *PCA3*-shRNA, or controls were s.c. administered into SCID mice. *PRUNE2* silencing and ectopic *PCA3* expression yielded markedly larger tumor xenografts than controls; in contrast, tumor growth was greatly diminished relative to

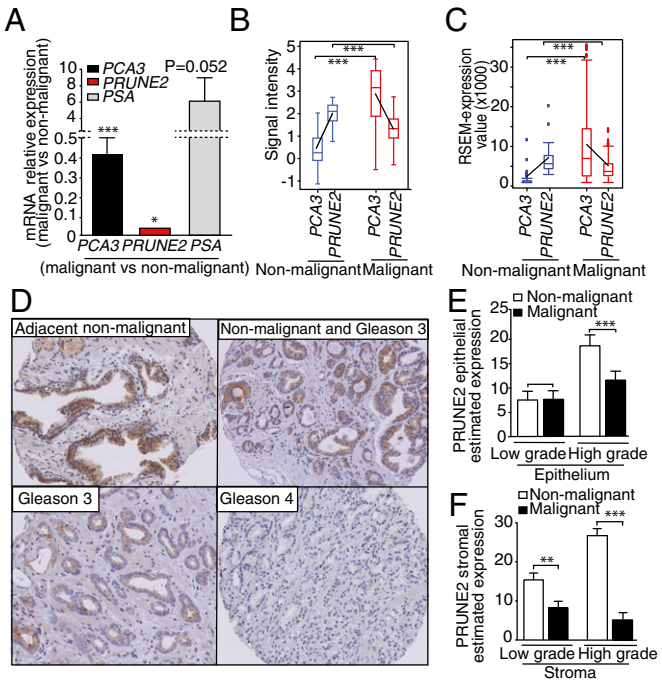

Fig. 5. PRUNE2/*PCA3* expression in prostate cancer patient samples. (*A*) Analysis of *PRUNE2* and *PCA3* mRNA levels in human prostate cancer samples ($n = 48$) vs. nonmalignant prostate tissue ($n = 9$). Malignant (M) vs. nonmalignant (NM) control is indicated. *PSA* served as a positive control for the qRT-PCR. In each case, *P* values are for M vs. NM. (*B*) *PCA3* and *PRUNE2* expression levels of cDNA microarrays from Oncomine. Blue, nonmalignant gland ($n = 29$); red, prostate tumor ($n = 115$). Box-and-whisker plots with the data are presented with the horizontal lines within boxes representing median signal intensity. Black lines depict the calculated slopes linking to average intensity values. (*C*) RSEM. Normalized RNA-Seq data from TCGA for *PCA3* and *PRUNE2* mRNA in NM (blue) or M (red) from human prostate specimens are shown. Box-and-whisker plots with the corresponding data are presented with the horizontal lines in the boxes representing the median signal intensity. Black lines depict the calculated slopes linking to average intensity values. (*D*) Human TMA of prostate cancer samples showing high-abundance of PRUNE2 in NM adjacent prostate tissue control compared with M. In each case, IHC staining (i.e., % extent of expression in cells) was analyzed. Magnification, 20×. (*E* and *F*) PRUNE2 estimated expression in the epithelium (*E*) or stromal (*F*) component of the tumor samples ($n = 145$) with low-grade ($n = 50$) and high-grade ($n = 95$) vs. NM adjacent control tissues ($n = 145$) in human prostate cancer specimens. Mean ± SD is shown. $^{**}P < 0.01$; $^{***}P < 0.001$.

controls when *PCA3* was silenced (Fig. 4 *A*–*C*). Consistently, we observed increased serum prostate-specific antigen (PSA) concentrations in SCID mice that received LNCaP cells with ectopic *PCA3* expression or *PRUNE2* silencing compared to controls (Fig. 4*D*). In vitro, and also in tumor xenograft models, expression of antisense *PCA3* (intron6-*PRUNE2*), which sequesters *PCA3*, decreased tumor growth in LNCaP but not in PC3 cells (Fig. 4 *E* and *F* and Fig. S8 *A* and *B*). Further, expression of ectopic PRUNE2 in LNCaP cells administered in SCID mice led to smaller tumors relative to controls (Fig. 4 *G* and *H*), illustrating the tumor suppressor activity of PRUNE2. Finally, silencing ADAR1, which increases PRUNE2 levels in LNCaP cells, reduced tumor cell proliferation in vitro and in vivo (Fig. 4 *I* and *J* and Fig. S11 *A*–*C*). These data show a functional role for the PRUNE2/*PCA3* regulatory axis in prostate cancer. To explore the potential of clinical application of these findings, we specifically targeted the *PCA3* sense strand with a modified siRNA (stealth RNAi-*PCA3*) serially administered to tumor-bearing mice with established prostate cancer xenografts. We observed tumor growth inhibition and serum PSA concentration reduction relative to scrambled siRNA control (Fig. 4 *K*–*N*). These results support the hypothesis that PRUNE2 expression has a functional tumor suppressive role in prostate cancer and suggest that the regulatory mechanism of PRUNE2 by *PCA3* is a molecular target for intervention.

Levels of *PCA3* and *PRUNE2* Inversely Correlate in Human Prostate Cancer Specimens. To determine the clinical relevance of our findings, we examined the expression of *PCA3* and *PRUNE2* in human prostate cancer. First, we performed qRT-PCR analysis on tumor RNA samples from prostate cancer patients ($n = 48$) and nonmalignant areas of the prostate ($n = 9$). *PRUNE2* mRNA expression was detected more often in non–tumor-containing compared with the tumor-containing areas of the prostate (Fig. 5*A*). In contrast, *PCA3* mRNA levels showed the opposite pattern, with high expression levels more frequently detected in tumors relative to nontumors, consistent with its role in the negative regulation of *PRUNE2*. To independently validate these clinical findings in silico, *PRUNE2* and *PCA3* expression levels were evaluated through Oncomine (19) in a large sample subset ($n = 144$) of primary nontreated prostate malignant tumors ($n = 115$) and nonmalignant prostate tissue ($n = 29$) (20). Although no statistically significant correlation with survival could be readily identified in this online dataset (20), a larger ongoing study is planned to fully address this question. Notably, to minimize variation, samples from prostate cancer-derived cell lines, metastatic lesions, and patients that received neoadjuvant therapy were excluded from the analysis. We next used The Cancer Genome Atlas (TCGA) as another unrelated large dataset ($n = 50$ nonmalignant control prostate samples; $n = 333$ prostate cancer samples) to validate the opposed expression between *PRUNE2* and *PCA3*. We found that low *PCA3* levels correlated with high *PRUNE2* levels in nonmalignant control prostate samples and vice

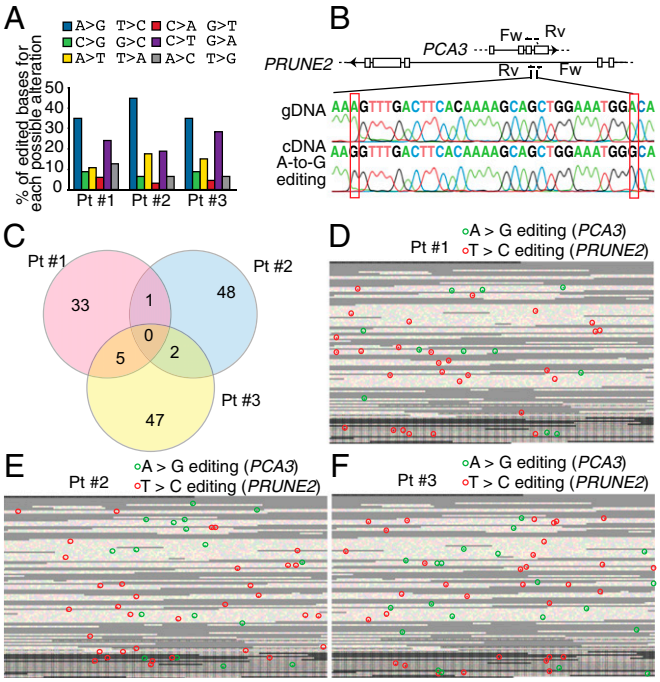

Fig. 6. RNA editing in specimens from prostate cancer patients. (*A*) All possible alterations, including putative editing sites, were determined as described for LNCaP cells and shown for each tumor sample. (*B*) A subset of editing sites suggested by large-scale sequencing was confirmed by PCR (with gDNA or cDNA as templates) followed by Sanger-sequencing. (*C*) Intersections of the putative edited sites among each independent patient sample are depicted. (*D*–*F*) Individual RNA editing maps of three prostate cancer patients are shown: Distribution of A > G (green)/T > C (red) sites over *PCA3* and intron6-*PRUNE2* pre-mRNA. Each square represents one individual base from the *PCA3* locus (23,112 nt). Black borders delimit the bases of the four annotated exons (3,923 nt). Repeats (RepeatMasker): gray.

versa in prostate cancer samples (Fig. 5 *B* and *C*). Finally, we also analyzed the protein expression pattern of PRUNE2 in a large series of clinically annotated primary prostate cancer specimens ($n = 145$), matched to adjacent histologically normal prostate tissue ($n = 145$). In each case, immunohistochemical (IHC) staining was compared between the epithelial and stromal cells within tumors to the nonmalignant epithelial and stromal cells from adjacent nonmalignant areas of the same specimen (Fig. 5 *D*–*F*). We found a higher abundance of PRUNE2 in nonmalignant vs. malignant areas. The inverse correlation between the native expression of *PRUNE2* and *PCA3* mRNA in clinical samples again supports a meaningful role for their coregulation and tumor suppression in human prostate cancer.

RNA Editing of *PCA3* and *PRUNE2* in Human Prostate Cancer Patients. We ultimately analyzed specimens obtained from index prostate cancer patients through RNA capture followed by next-generation sequencing and detected the presence of RNA editing (Fig. 6*A*), which was subsequently confirmed by classic Sanger sequencing (Fig. 6*B*) of genomic and cDNA clones from the same index patients. Bioinformatics demonstrated A > G/T > C alterations as the most frequent substitutions and data indicative of A-to-I editing in both *PCA3* and *PRUNE2* pre-mRNA strands, with no clear editing hotspots identified in human tumor samples (Fig. 6*C*). The editing maps provided for all patients show a similar distribution of alterations for both RNA strands, suggesting the interaction of the pre-mRNAs of both *PCA3* and *PRUNE2* transcripts (Fig. 6*D*).

Discussion

lncRNAs have recently emerged as central regulators of gene expression in various biological settings, but only a few have known functional roles in human prostate cancer (1, 4, 5, 21–24). Here we present extensive data that are consistent with an antisense intronic lncRNA (i.e., *PCA3*) that acts by an ADAR-mediated RNA editing mechanism to down-regulate its target gene (i.e., *PRUNE2*). In this study, we establish the functional attributes of *PCA3* as a trans-dominant negative oncogene that inactivates the unrecognized tumor suppressor gene *PRUNE2* at the RNA level through an ADAR-mediated mechanism; such a remarkable regulatory unit located in a single genetic locus appears unique to human mammalian cells. Notably, the genomic region encompassing *PRUNE2* contains several alternatively spliced isoforms (25–28), one of which is ∼3 kb shorter than the *PRUNE2* full-length sequence identified here (presumably the canonical gene) and is found in human adult nerve cells (25), with a related mouse brain-specific isoform (26); thus, other tissue-specific isoforms with different functions may perhaps exist. Tumor suppressor genes have long been shown to affect cancer growth in the classic two-hit hypothesis (29, 30). More recently, it became clear that even partial inactivation of tumor suppressors contribute critically to tumorigenesis (31), as illustrated here. In sum, we show a striking function for the clinically well-established *PCA3* marker that will lead to translational applications in human prostate cancer.

Materials and Methods

Details can be found in *SI Materials and Methods*. *PCA3* and *PRUNE2* sequence analyses were evaluated from cDNA microarray with Oncomine (19) or RNA-seq data from TCGA; expression was calculated by RNA-Seq by expectation maximization (RSEM) (32). Cell fractionation, nuclear RNA analysis, and immunoprecipitation/immunoblot were performed as previously described (13). siRNA and shRNA were custom-ordered against PCA3 or PRUNE2 (Table S1), respectively, and transfected into tumor cells (Ambion). Custom-ordered siRNAs against *PCA3* (Tables S1 and S2) were transfected into tumor cells with the NeoFX transfection reagent (Ambion). RNA FISH and confocal microscopy RNAs were performed to detect *PCA3* and *PRUNE2*. Cell culture and functional assays (cell proliferation, viability, adhesion, migration, soft agar colony formation, and tumor cell-derived spheroids) were performed. Tumor-bearing mouse models are described elsewhere (11). All animal experimentation was reviewed and approved by the Institutional Animal Care and Use Committee of the University of Texas M.D. Anderson Cancer Center (MDACC). Experiments with human samples were reviewed and approved by the Clinical Research Committee and by the institutional review board (IRB) at MDACC. All human specimens were obtained after the patients provided written informed consent under an IRB-approved experimental protocol. Total RNA samples purified from tumors from human prostate cancer patients were also obtained from the Tumor Bank at A.C. Camargo Cancer Center after IRB approval.

ACKNOWLEDGMENTS. This work was supported by National Institutes of Health Grants CA90270 (to R.P. and W.A.) and CA95616 (W.K.C.), Angel-Works, Gilson-Longenbaugh Foundation, Prostate Cancer Foundation (W.A. and R.P.), Fundação de Amparo à Pesquisa do Estado de São Paulo, and Associação Beneficente Alzira Denise Hertzog Da Silva (E.D-N.).

1. Walsh AL, Tuzova AV, Bolton EM, Lynch TH, Perry AS (2014) Long noncoding RNAs and prostate carcinogenesis: The missing 'linc'? *Trends Mol Med* 20(8):428–436.
2. Bussemakers MJG, et al. (1999) DD3: A new prostate-specific gene, highly overexpressed in prostate cancer. *Cancer Res* 59(23):5975–5979.
3. Wei JT, et al. (2014) Can urinary PCA3 supplement PSA in the early detection of prostate cancer? *J Clin Oncol* 32(36):4066–4072.
4. Esteller M (2011) Non-coding RNAs in human disease. *Nat Rev Genet* 12(12):861–874.
5. Fatica A, Bozzoni I (2014) Long non-coding RNAs: New players in cell differentiation and development. *Nat Rev Genet* 15(1):7–21.
6. Geisler S, Coller J (2013) RNA in unexpected places: Long non-coding RNA functions in diverse cellular contexts. *Nat Rev Mol Cell Biol* 14(11):699–712.
7. Machida T, et al. (2006) Increased expression of proapoptotic BMCC1, a novel gene with the BNIP2 and Cdc42GAP homology (BCH) domain, is associated with favorable prognosis in human neuroblastomas. *Oncogene* 25(13):1931–1942.
8. Clarke RA, et al. (2009) New genomic structure for prostate cancer specific gene PCA3 within BMCC1: Implications for prostate cancer detection and progression. *PLoS ONE* 4(3):e4995.
9. Lavin MF, Clarke R, Gardiner RA (2009) Differential expression of PCA3 and BMCC1 in prostate cancer. *Prostate* 69(16):1713–1714, author reply 1715.
10. Salagierski M, et al. (2010) Differential expression of PCA3 and its overlapping PRUNE2 transcript in prostate cancer. *Prostate* 70(1):70–78.
11. Lee YC, et al. (2011) BMP4 promotes prostate tumor growth in bone through osteogenesis. *Cancer Res* 71(15):5194–5203.
12. Bass BL (2002) RNA editing by adenosine deaminases that act on RNA. *Annu Rev Biochem* 71:817–846.
13. Chen L-L, DeCerbo JN, Carmichael GG (2008) Alu element-mediated gene silencing. *EMBO J* 27(12):1694–1705.
14. Mallela A, Nishikura K (2012) A-to-I editing of protein coding and noncoding RNAs. *Crit Rev Biochem Mol Biol* 47(6):493–501.
15. Ferreira LB, et al. (2012) PCA3 noncoding RNA is involved in the control of prostate-cancer cell survival and modulates androgen receptor signaling. *BMC Cancer* 12:507.
16. Soh UJ, Low BC (2008) BNIP2 extra long inhibits RhoA and cellular transformation by Lbc RhoGEF via its BCH domain. *J Cell Sci* 121(Pt 10):1739–1749.
17. Galasso A, Zollo M (2009) The Nm23-H1-h-Prune complex in cellular physiology: A 'tip of the iceberg' protein network perspective. *Mol Cell Biochem* 329(1-2):149–159.
18. Basile JR, Gavard J, Gutkind JS (2007) Plexin-B1 utilizes RhoA and Rho kinase to promote the integrin-dependent activation of Akt and ERK and endothelial cell motility. *J Biol Chem* 282(48):34888–34895.
19. Rhodes DR, et al. (2004) ONCOMINE: A cancer microarray database and integrated data-mining platform. *Neoplasia* 6(1):1–6.
20. Taylor BS, et al. (2010) Integrative genomic profiling of human prostate cancer. *Cancer Cell* 18(1):11–22.
21. Cech TR, Steitz JA (2014) The noncoding RNA revolution-trashing old rules to forge new ones. *Cell* 157(1):77–94.
22. Guttman M, et al. (2011) lincRNAs act in the circuitry controlling pluripotency and differentiation. *Nature* 477(7364):295–300.
23. Mercer TR, Dinger ME, Mattick JS (2009) Long non-coding RNAs: Insights into functions. *Nat Rev Genet* 10(3):155–159.
24. Ponting CP, Oliver PL, Reik W (2009) Evolution and functions of long noncoding RNAs. *Cell* 136(4):629–641.
25. Iwama E, et al. (2011) Cancer-related PRUNE2 protein is associated with nucleotides and is highly expressed in mature nerve tissues. *J Mol Neurosci* 44(2):103–114.
26. Arama J, et al. (2012) Bmcc1s, a novel brain-isoform of Bmcc1, affects cell morphology by regulating MAP6/STOP functions. *PLoS ONE* 7(4):e35488.
27. Harris JL, et al. (2013) BMCC1 is an AP-2 associated endosomal protein in prostate cancer cells. *PLoS ONE* 8(9):e73880.
28. Pan CQ, Low BC (2012) Functional plasticity of the BNIP-2 and Cdc42GAP Homology (BCH) domain in cell signaling and cell dynamics. *FEBS Lett* 586(17):2674–2691.
29. Knudson AG, Jr (1971) Mutation and cancer: Statistical study of retinoblastoma. *Proc Natl Acad Sci USA* 68(4):820–823.
30. Cavenee WK, et al. (1983) Expression of recessive alleles by chromosomal mechanisms in retinoblastoma. *Nature* 305(5937):779–784.
31. Berger AH, Knudson AG, Pandolfi PP (2011) A continuum model for tumour suppression. *Nature* 476(7359):163–169.
32. Li B, Dewey CN (2011) RSEM: Accurate transcript quantification from RNA-Seq data with or without a reference genome. *BMC Bioinformatics* 12:323.